Crystal Structure and Magnetism of the Linear-Chain Copper Oxides $Sr_5Pb_{3-x}Bi_xCuO_{12}$

K. Yamaura*
Advanced Materials Laboratory, National Institute for Materials Science, 1-1 Namiki, Tsukuba, Ibaraki 305-0044, Japan and Japan Science and Technology Corporation, Kawaguchi, Saitama 332-0012, Japan

Q. Huang
NIST Center for Neutron Research, National Institute of Standards and Technology, Gaithersburg, Maryland 20899 and Department of Materials and Nuclear Engineering, University of Maryland, College Park, Maryland 20742

E. Takayama-Muromachi
Advanced Materials Laboratory, National Institute for Materials Science, 1-1 Namiki, Tsukuba, Ibaraki 305-0044, Japan

(Dated: 18 June 2001)

The title quasi-1D copper oxides ($0 \leq x \leq 0.4$) were investigated by neutron diffraction and magnetic susceptibility studies. Polyhedral CuO_4 units in the compounds were found to comprise linear-chains at inter-chain distance of approximately 10 Å. The parent chain compound ($x = 0$), however, shows less anisotropic magnetic behavior above 2 K, although it is of substantially antiferromagnetic ($\mu_{\rm eff}$ = 1.85 $\mu_{\rm B}$ and $\Theta_{\rm W}$ = -46.4 K) spin-chain system. A magnetic cusp gradually appears at about 100 K in T vs χ with the Bi substitution. The cusp ($x = 0.4$) is fairly characterized by and therefore suggests the spin gap nature at $\Delta/k_{\rm B} \sim 80$ K. The chain compounds hold electrically insulating in the composition range.

PACS numbers: 75.50.-y, 81.40.Rs

I. INTRODUCTION

A variety of Cu(II) based linear-chain oxides is known such as $Ca_4Cu_5O_{10}$, Li_2CuO_2, $CuGeO_3$, Sr_2CuO_3, $SrCuO_2$, and $Y_2Ca_2Cu_5O_{10}$, and indeed one dimensional Heisenberg antiferromagnetism was observed in those materials [1]. Studies on the copper oxides play an important role in research on the one dimensional electronic systems, raising and settling fundamental issues as to the nature of quasi-particles and electron correlations in condensed matter [1]. We have recently been studying copper based chain materials in order to find additional systems showing correlations among their magnetic and electrical properties and crystal structure.

In this paper we report the crystal structure and magnetic properties of the linear-chain copper oxides $Sr_5Pb_{3-x}Bi_xCuO_{12}$ ($0 \leq x \leq 0.4$). In the parent compound $Sr_5Pb_3CuO_{12}$, distorted CuO_4 units are linearly connected by sharing a conner-oxygen [2, 3]. One-dimensionally anisotropic magnetic properties were then expected to $Sr_5Pb_3CuO_{12}$ because the copper ion has spin-1/2 electronic configuration and the principal magnetic bond Cu–O–Cu ($\sim 165°$) in chain is supposed antiferromagnetic [4]. Experimental studies, however, seemed not to be focused on magnetism of this compound probably because insufficient quality of the so-far samples and relatively high degree of structural disorder [2, 3]. Even the most high quality sample was made at copper-rich starting composition Sr:Pb:Cu=3:2:1 rather than copper-stoichiometric composition [3]. The sample quality level was acceptable for a regular structural study, but rather unsuitable for detailed magnetic studies because the sample should have unknown magnetic impurities [3]. The magnetism of the quasi-1D compound $Sr_5Pb_3CuO_{12}$ remained ambiguous.

In this study, further improvement of quality of the copper-stoichiometric sample of $Sr_5Pb_3CuO_{12}$ and partial Bi substitution for Pb, i.e. $Sr_5Pb_{3-x}Bi_xCuO_{12}$, up to $x = 0.4$ were achieved in single-phase polycrystalline form, followed by investigations by neutron diffraction and magnetic susceptibility studies. We found the quasi-1D compound $Sr_5Pb_3CuO_{12}$ shows Curie-Weiss-type magnetism even at low temperature (> 2 K), and at the composition $Sr_5Pb_{2.6}Bi_{0.4}CuO_{12}$ a finite energy gap ($\Delta/k_{\rm B} \sim 80$ K) in magnetic system was suggested.

II. EXPERIMENTAL

The polycrystalline single-phase samples were prepared by high-temperature ceramic synthesis technique. Mixtures of $SrCO_3$, PbO, Bi_2O_3, and CuO with the ratio Sr:Pb:Bi:Cu = $5{:}3-x{:}x{:}1$ (x = 0, 0.1, 0.2, 0.3, 0.4, 0.6, 0.8, 1.0) were heated at 800 °C for 15 hours in air. After the initial treatment, grinding and heating in air were repeated at 800 °C, followed by those at 850 and 900 °C for 95 hours in total. The samples were then ground and molded into pellets, and again heated in air

*E-mail:YAMAURA.Kazunari@nims.go.jp

at 950 °C for 45 hours. The heating at 950 °C in either nitrogen or oxygen instead of air results in poor quality of final productions. Subsequently, the sintered pellets were annealed at 500 °C in compressed (100 MPa) gas, 20 % oxygen in argon, for 5 hours. The quality of the final productions were quite sensitive to the highest heating temperature. Dense alumina crucibles were employed to hold the samples in the synthesis procedure. The magnetic properties of the samples were studied by a commercial apparatus between 2 and 390 K. The highest applied magnetic field was 55 kOe. All of the pellets thus obtained were electrically highly insulating.

Powder x-ray diffraction with CuKα radiation at room temperature was employed to characterize the samples and found a part of those ($x = 0 - 0.4$) was single-phase within the sensitivity of the technique ($\sim$ 1 %). Composition dependence of lattice constants and volume of the hexagonal unit cell are plotted in Fig.1. Linear dependence in V, c vs x, and x independence of a are clearly seen, indicates the solid solution is formed. The end members, $Sr_5Pb_3CuO_{12}$ and $Sr_5Pb_{2.6}Bi_{0.4}CuO_{12}$, were then selected for further crystal structure studies by neutron diffraction at 10 and 295 K. The neutron diffraction data were obtained by the BT-1 high-resolution powder diffractometer at the NIST Center for Neutron Research. A Cu(311) monochromator was employed to produce a coherent neutron beam ($\lambda = 1.5401$ Å) with 15′, 20′, and 7′ collimators before and after the monochromator, and after the sample, respectively. The intensity of diffracted neutron beam was measured between 3 and 160 degrees at each 0.05 degrees step in 2Θ. Crystal structure parameters of the copper oxides were then refined to a high degree of agreement by calculations with the intensity and angle data on the program GSAS [5]. Neutron scattering amplitudes for the elements in the refinements were set to 0.702, 0.940, 0.853, 0.772, and 0.581 ($\times 10^{-12}$) cm for Sr, Pb, Bi, Cu, and O, respectively [5].

III. RESULTS AND DISCUSSIONS

A. Crystal Structure

At first, oxygen stoichiometry and crystal structure of the $x = 0$ sample were investigated. A crystal structure model [$P\bar{6}2m$, $a = 10.1089(6)$ Å and $c = 3.5585(2)$ Å] previously proposed for $Sr_5Pb_3CuO_{12}$, of which the powder sample was prepared at the composition Sr:Pb:Cu=3:2:1 [3], was tested. In the top panel in Fig.2, the observed profile is presented with the calculated one. As you can see, all observed peaks are clearly reproduced at 4–5 % levels in agreement factors, indicating the qualities of the sample and the refinement. The structural model is valid for the present compound prepared at the correct composition. Lattice constants of the hexagonal unit cell ($P\bar{6}2m$) are $a = 10.1297(2)$ Å and $c = 3.559\,80(7)$ Å for $Sr_5Pb_3CuO_{12}$ at 295 K; there are insignificant difference between lattice parameters for the 321 and present samples (0.2 % and 0.04 % in a and c parameters, respectively). The structure parameters are summarized in Table I. The occupancy factors of oxygen in the normally occupied sites, O(2) and O(3), were refined to within one standard deviation of 1.00, and the sites were therefore taken to be fully occupied. The occupancy factors in the partially occupied sites, O(1), O(4) and O(5), are slightly larger than 2/3, 1/12 and 1/12, respectively, which are expected when the compound is oxygen-stoichiometric at 12 moles of oxygen per formula unit. Magnetometric study of the sample indicates the valence state of copper is fairly close to +2 as discussed later, supports the oxygen-stoichiometric composition $Sr_5Pb_3CuO_{12}$. Because the occupancy factors are highly correlated with the thermal-displacement parameters, which are unusual due to the remarkably low levels of oxygen occupancy, and complicated local structure in chain, the oxygen occupancy factors are presumed slightly overestimated. Unreasonable values for B_{11} of O(4) were probably gained due to the same reasons. The composition of the sample is then $Sr_5Pb_3CuO_{12}$ or possibly somewhat oxygen-superstoichiometric.

The neutron diffraction profile of the $x = 0.4$ sample at 295 K is presented in the bottom panel in Fig.2 as well as that of $x = 0$ sample. The obtained structure parameters at 295 and 10 K are listed and compared with those for the $x = 0$ sample in Table I. The qualities of the sample of $Sr_5Pb_{2.6}Bi_{0.4}CuO_{12}$ and the refinement are as good as those achieved for $Sr_5Pb_3CuO_{12}$. Lattice constants of the hexagonal unit cell ($P\bar{6}2m$) are $a = 10.1236(2)$ Å and $c = 3.541\,82(6)$ Å for $Sr_5Pb_{2.6}Bi_{0.4}CuO_{12}$ at 295 K, and $a = 10.1042(2)$ Å and $c = 3.534\,90(6)$ Å at 10 K. The oxygen quantity is independent on the Bi doping level; no significant deference in oxygen occupancy factors was detected between both the samples. On the assumption that Pb and Bi valences are +4 and +3, respectively, the formal copper valence of $Sr_5Pb_{2.6}Bi_{0.4}CuO_{12}$ should be +2.4, does not meet the expectation from the observed effective Bohr magneton as shown later. Partial increment of the Bi valence to +5 therefore probably occur.

Schematic structural view for $Sr_5Pb_{2.6}Bi_{0.4}CuO_{12}$ is presented as a representative of the solid solution in Fig.3, based on the structure parameters at 295 K. The Bi doped compound retains the linear-chain structure basis, in which copper–oxygen polyhedra form chains at inter-chain distance of approximately 10 Å. The local structure of the chain is highly complicated as indicated in Fig.4a, where all possible oxygen and copper positions are indicated. In Fig.4b, probable local arrangements of CuO_4 units include a misordering of copper atom (third one from the left side) is shown by precluding coordinations of copper and oxygen resulting in intolerably short bond distances. On the other hand, the 4–18 and 2–10 Å^2 thermal displacement parameters for Cu and O(1), respectively, are also unusual, indicating probable presence of local displacements of Cu and O(1) along $c-$axis (Fig.4a) and frequent occurrence of the irregular copper atom arrangement in local. Due to the compli-

cated chain structure, a comparison between the structure data at 10 and 295 K for $Sr_5Pb_{2.6}Bi_{0.4}CuO_{12}$ does not give a significant contribution to detect possible local lattice distortions associated with magnetism as found in $CuGeO_3$ [6]. Further crystal structure investigations into $Sr_5Pb_{2.6}Bi_{0.4}CuO_{12}$ include microscopic studies and structure modulation analysis should be interesting.

B. Magnetic Properties

The temperature dependence of the magnetic susceptibility of $Sr_5Pb_{3-x}Bi_xCuO_{12}$ ($0 \leq x \leq 0.4$) was measured at magnetic field of 10 kOe. Those data are presented in Fig.5 as $\chi - \chi_0$ vs. T and $1/(\chi - \chi_0)$ vs. T plots (χ_0 is temperature-independent portion). The magnetic field dependence of the magnetization at 5 K of the selected samples (x =0 and 0.4) are shown in Fig.6a. In the enough high temperature region above 200 K, the magnetic data are expected free from any of magnetic ordering contributions either long or short range because the characteristic magnetic cusp was found far below the temperature region. The Weiss temperature ($\Theta_{\rm W}$), χ_0, and the effective Bohr magneton ($\mu_{\rm eff}$) were estimated by fitting the Curie-Weiss law to the data above 200 K. The solid lines in Fig.5 indicate the fits, and those magnetic parameters estimated are presented in Fig.6b. The formula for the fitting by least-squares method was

$$\chi(T) = \frac{N\mu_{\rm eff}^2}{3k_{\rm B}(T-\Theta_{\rm W})} + \chi_0 \quad (T > 200\ {\rm K}), \tag{1}$$

where $k_{\rm B}$ and N are Boltzmann and Avogadro's constants, respectively.

The Weiss temperatures estimated for $Sr_5Pb_{3-x}Bi_xCuO_{12}$ are characteristic of antiferromagnetic interactions (Fig.6b), and the absolute value tends to be gradually elevated as the Bi doping level increases. The χ_0 in the composition range is almost constant, $\sim -6 \times 10^{-4}$ emu/mol Cu, which is remarkable approximately one magnitude larger than the values for the other chain structure copper oxides [1]. This fact is probably due to the unusually large number of diamagnetic elements per copper (20 moles per mole Cu) [7], therefore we decided not to make further concerns on this issue. The effective Bohr magneton is slightly above 1.73 $\mu_{\rm B}$, calculated from the ideal electronic configuration of Cu(II) ($3d^9$, t_{2g}^6 e_g^3, $S = 1/2$) using the formula $\mu_{\rm eff} = 2\sqrt{S(S+1)}$ $\mu_{\rm B}$. The effective g-value are expected different somewhat rather than 2.00 if the valence of copper is fixed at +2.00 in the composition range. By considering the negative value of Weiss temperature and the effective Bohr magneton, it is concluded that antiferromagnetic interaction is dominant between the nearest neighbor spin–1/2 magnetic moments in chain of $Sr_5Pb_{3-x}Bi_xCuO_{12}$. Ferromagnetic interactions in $Sr_5Pb_{3-x}Bi_xCuO_{12}$ are insignificant because ferromagnetic characters such as hysteresis and spontaneous moments were not found at all in the M vs. H curves (Fig.6a).

Magnetic susceptibility of the antiferromagnetic linear-chain system is divided into three terms [8]:

$$\chi(T) = (1-f)\chi_{\rm 1D}(T) + f\chi_{\rm C}(T) + \chi_0, \tag{2}$$

where f is level of the Curie term [$\chi_{\rm C}(T)$], and $\chi_{\rm 1D}(T)$ stands for the intrinsic linear-chain magnetic susceptibility. To further analyze the $x = 0.4$ data, which are most influenced by the linear-chain magnetism as the cusp appears at $\sim$ 80 K, the low temperature quasi-Curie component was subtracted (Fig.7). The Eq.1 with $\Theta'_{\rm W}$ instead of $\Theta_{\rm W}$ was employed to estimate the quasi-Curie component by fitting to the original data below 8 K as indicated by the broken curve in Fig.7 ($f \sim 13.3$ % and $\Theta'_{\rm W} = -0.66$ K). As the chemical impurity level of the sample is less than 1 %, it is concluded that the nearly 13 % of magnetic moments in $Sr_5Pb_{2.6}Bi_{0.4}CuO_{12}$ formally contribute to form the low temperature quasi-Curie term. Origins to produce the almost free-spins, which yield the nearly zero Weiss temperature, are possibly associated with the local structural disorders, which may cut and cause end of chains. The detailed analysis of the substantial amount of free-spins in chain using further experimental studies is left for future works.

After the Curie term subtraction, character of the $\chi_{\rm 1D}(T)$ term becomes clear; it goes to zero on cooling. At present we presume that the particular magnetism is due to an energy gap between magnetic ground and excited states, as found in the spin-ladder and the alternating-exchange linear-chain materials [1, 8]. The formula proposed for spin gap system at $T \ll \Delta/k_{\rm B}$ [9],

$$\chi_{\rm 1D}(T) \sim \frac{1}{\sqrt{T}} \exp\left(-\frac{\Delta}{T}\right), \tag{3}$$

was applied on the data below 35 K, as shown in the inset in Fig.7, and found that the possible energy gap ($\Delta/k_{\rm B}$) is approximately 80 K. An alternative fit to a model in which there are Curie-Weiss and Heisenberg Bonner-Fisher components [10] was unlikely at all. Even at the best result (dotted curve at S =1/2, $g = 2$, $\Theta'_{\rm W}$ = -0.19 K, f = 23.6 %, and $J_{\rm eff}/k_{\rm B}$= 72.4 K) it was too poor to reproduce the original data.

Alternating antiferromagnetic spin-chain system has been intensively investigated in $(VO)_2P_2O_7$ and $Cu(NO_3)_2{\cdot}2.5H_2O$ [8, 11, 12, 13]. The model was tested on the present linear-chain material $Sr_5Pb_{2.6}Bi_{0.4}CuO_{12}$ by applying the applicable formula to the data above 60 K, which has three independent variable parameters J_1, α ($= J_2/J_1$) and $g-$value, where J_1 and J_2 are antiferromagnetic exchange constants alternating along chain ($J_1 \geq J_2 \geq 0$) [14, 15]. The best fit was obtained at $J_1/k_{\rm B}$ = 183 K, α = 0.58 and g = 2.22, as shown in Fig.7 (fat solid curve). Thus, the magnetic cusp temperature was calculated 115 K from the formula $\sim 0.63J_1/k_{\rm B}$, which is expected almost independent on α [16], and the spin gap 77 K from $\sim J_1 - J_2$ [17], those in fact match well

with the observations. The alternating spin chain model at $\alpha \sim 0.6$ is, therefore, the most probable model to account for the character of $\chi_{1D}(T)$ of $Sr_5Pb_{2.6}Bi_{0.4}CuO_{12}$ if the spin gap nature is prime essential in the magnetism of this compound. Further investigations employing probes more sensitive to the microscopic magnetic environment, such as NMR studies, would play a significant role to figure out the magnetic ground state and the excitation. As a clue to further elucidate the possible spin gap nature of $Sr_5Pb_{2.6}Bi_{0.4}CuO_{12}$, inelastic-neutron-scattering study would also be expected particularly if a single crystal becomes available.

IV. CONCLUSION

It was found that the substantial Bi substitution for Pb in $Sr_5Pb_3CuO_{12}$ plays a key role to profile the one dimensional antiferromagnetic feature, without a significant influence on the electrical conductivity. At $x = 0.4$, the alternating magnetic interactions at $\alpha \sim 0.6$ was strongly suggested, which potentially produce spin-singlet ground state with approximately 80 K spin-gap. There are two major models to explain a cusp in T vs χ in antiferromagnetic linear-chain system as far as we know. As already described the one does not match ultimately with the present magnetic data, and the other one reaches sufficiently convincible level in the fitting study; these facts imply the spin gap nature in the $x = 0.4$ chain compound. Because conclusive evidence is not provided yet about the probable spin gap, further investigations include theoretical point of view into the Bi doped compound would be of interest. The alteration possibly depend on the Bi doping level, which modifies the local magnetic environments. It is not figure out yet how the doping improves the local magnetic environment around copper and what produces the low-temperature Curie term. Further Bi doping would probably be favorable to obtain credible information about the issues and make clear nature of the magnetism of the title spin chain compounds. As an electrical carrier doping to spin gap system would be of great interest, further studies of a variety of chemical substitutions for $Sr_5Pb_3CuO_{12}$ are in progress.

Acknowledgments

We are grateful to M. Isobe (AML/NIMS) for helpful discussions. This research was supported in part by the Multi Core Project administrated by Ministry of Education, Culture, Sports, Science, and Technology of Japan.

[1] M. Imada, A. Fujimori, and Y. Tokura, Rev. Mod. Phys. **70**, 1039 (1998).
[2] J.S. Kim, X.X. Tang, A. Manthiram, J.S. Swinnea, and H. Steinfink , J. Solid State Chem. **85**, 44 (1990).
[3] T.G.N. Babu and C. Greaves, J. Solid State Chem. **95**, 417 (1991).
[4] Y. Mizuno, T. Tohyama, and S. Maekawa, T. Osafune, N. Motoyama, H. Eisaki, and S. Uchida, Phys. Rev. B **57**, 5326 (1998).
[5] A.C. Larson and R.B. Von Dreele, Los Alamos National Laboratory Report No. LAUR086-748 (1990).
[6] J.P. Pouget, L.P. Regnault, M. Ain, B. Hennion, J.P. Renard, P. Veillet, G. Dhalenne, and A. Revcolevschi, Phys. Rev. Lett. **72**, 4037 (1994).
[7] J.H. Van Vleck, *The Theory of Electronic and Magnetic Susceptibility*, (Oxford Univ. Press, 1932).
[8] D.C. Johnston, R.K. Kremer, M. Troyer, X. Wang, A. Klümper, S.L. Bud'ko, A.F. Panchula, and P.C. Canfield, Phys. Rev. B **61**, 9558 (2000).
[9] M. Troyer, H. Tsunetsugu, and D. Würtz, Phys. Rev. B **50**, 13 515 (1994).
[10] J.C. Bonner and M.E. Fisher, Phys. Rev. **135**, A640 (1964).
[11] J.C. Bonner, S.A. Friedberg, H. Kobayashi, D.L. Meier, and H.W.J. Blöte, Phys. Rev. B **27**, 248 (1983).
[12] D.C. Johnston, J.W. Johnson, D.P. Goshorn, and A.J. Jacobson, Phys. Rev. B **35**, 219 (1987).
[13] T. Barnes and J. Riera, Phys. Rev. B **50**, 6817 (1994).
[14] J.W. Hall, W.E. Marsh, R.R. Weller, and W.E. Hatfield, Inorg. Chem. **20**, 1033 (1981).
[15] W.E. Hatfield, J. Appl. Phys. **52**, 1985 (1981).
[16] J.C. Bonner, H.W.J. Blöte, J.W. Bray, and I.S. Jacobs, J. Appl. Phys. **50**, 1810 (1979).
[17] P.R. Hammar, D.H. Reich, C. Broholm, and F. Trouw, Phys. Rev. B **57**, 7846 (1998).

TABLE I: Structure parameters of $Sr_5Pb_3CuO_{12}$ at 295 K (first line), $Sr_5Pb_{2.6}Bi_{0.4}CuO_{12}$ at 295 K (second line), and $Sr_5Pb_{2.6}Bi_{0.4}CuO_{12}$ at 10 K (third line). Space group for those is $P\bar{6}2m$. The lattice parameters are $a = 10.1297(2)$ Å and $c = 3.559\ 80(7)$ Å for $Sr_5Pb_3CuO_{12}$, $a = 10.1236(2)$ Å and $c = 3.541\ 82\ (6)$ Å for $Sr_5Pb_{2.6}Bi_{0.4}CuO_{12}$ at 295 K, and $a = 10.1042(2)$ Å and $c = 3.534\ 90(6)$ Å for $Sr_5Pb_{2.6}Bi_{0.4}CuO_{12}$ at 10 K.

Atom	Site	x	y	z	n
Sr(1)	2d	1/3	2/3	1/2	1
		1/3	2/3	1/2	1
		1/3	2/3	1/2	1
Sr(2)	3g	0.7019(3)	0	1/2	1
		0.7017(3)	0	1/2	1
		0.7027(2)	0	1/2	1
Pb/Bi	3f	0.3407(2)	0	0	1
		0.3381(2)	0	0	1
		0.3378(2)	0	0	1
Cu	2e	0	0	0.3360(39)	0.5
		0	0	0.3275(43)	0.5
		0	0	0.3351(37)	0.5
O(1)	3g	0.1747(6)	0	1/2	0.771(17)
		0.1767(5)	0	1/2	0.785(16)
		0.1777(4)	0	1/2	0.755(14)
O(2)	3g	0.4619(3)	0	1/2	1
		0.4614(3)	0	1/2	1
		0.4610(2)	0	1/2	1
O(3)	6j	0.2371(2)	0.4432(3)	0	1
		0.2369(2)	0.4435(3)	0	1
		0.2374(1)	0.4439(2)	0	1
O(4)	6i	0.1383(13)	0	0.2471(41)	0.109(4)
		0.1384(17)	0	0.2085(75)	0.105(4)
		0.1424(13)	0	0.2396(48)	0.107(3)
O(5)	6i	0.9592(11)	0	0.9238(35)	0.109(4)
		0.9587(14)	0	0.9300(89)	0.105(4)
		0.9588	0	0.9301	0.107(3)

	B_{11} (Å^2)	B_{22} (Å^2)	B_{33} (Å^2)	B_{12} (Å^2)	B_{13} (Å^2)	B_{23} (Å^2)
Sr(1)	1.43(10)	$= B_{11}$[Sr(1)]	1.56(14)	0.717(49)	0	0
	1.43(11)	$= B_{11}$[Sr(1)]	1.25(15)	0.719(54)	0	0
	0.861(78)	$= B_{11}$[Sr(1)]	0.54(11)	0.430(39)	0	0
Sr(2)	1.30(9)	0.723(97)	0.825(99)	0.362(49)	0	0
	1.16(8)	0.83(10)	0.85(10)	0.414(51)	0	0
	0.702(64)	0.427(84)	0.506(83)	0.213(42)	0	0
Pb/Bi	0.487(61)	0.962(90)	1.73(6)	0.481(45)	0	0
	0.629(57)	0.873(88)	1.19(6)	0.437(44)	0	0
	0.386(46)	0.369(69)	0.804(47)	0.184(34)	0	0
Cu	9.39(61)	$= B_{11}$(Cu)	13.4(14)	4.70(31)	0	0
	9.24(65)	$= B_{11}$(Cu)	17.9(20)	4.62(32)	0	0
	8.36(50)	$= B_{11}$(Cu)	16.1(16)	4.18(25)	0	0
O(1)	3.66(31)	3.09(38)	8.11(56)	1.54(19)	0	0
	2.46(24)	2.20(33)	9.33(59)	1.10(17)	0	0
	2.41(21)	1.66(28)	6.57(42)	0.83(14)	0	0
O(2)	1.74(11)	2.51(14)	0.38(11)	1.26(7)	0	0
	1.43(11)	2.99(15)	0.63(12)	1.50(8)	0	0
	0.743(82)	1.69(11)	0.473(98)	0.845(54)	0	0
O(3)	0.838(87)	1.41(10)	1.45(8)	0.402(95)	0	0
	0.820(84)	1.61(10)	1.34(8)	0.591(90)	0	0
	0.362(67)	0.770(85)	0.960(65)	0.033(69)	0	0
O(4)	-0.91(42)	1.33(53)	2.16(69)	0.67(26)	2.46(33)	0
	0.21(45)	4.63(86)	6.7(15)	2.32(43)	2.23(61)	0
	-0.36(35)	2.27(54)	3.49(82)	1.13(27)	2.13(30)	0
O(5)	$= B_{11}$[O(4)]	$= B_{22}$[O(4)]	$= B_{33}$[O(4)]	$= B_{12}$[O(4)]	$= B_{13}$[O(4)]	$= B_{23}$[O(4)]
	$= B_{11}$[O(4)]	$= B_{22}$[O(4)]	$= B_{33}$[O(4)]	$= B_{12}$[O(4)]	$= B_{13}$[O(4)]	$= B_{23}$[O(4)]
	$= B_{11}$[O(4)]	$= B_{22}$[O(4)]	$= B_{33}$[O(4)]	$= B_{12}$[O(4)]	$= B_{13}$[O(4)]	$= B_{23}$[O(4)]

$R_p =$	4.03 %	$R_{wp} =$	4.90 %	$\chi^2 =$	1.144
	4.35 %		5.30 %		1.184
	4.34 %		5.23 %		1.510

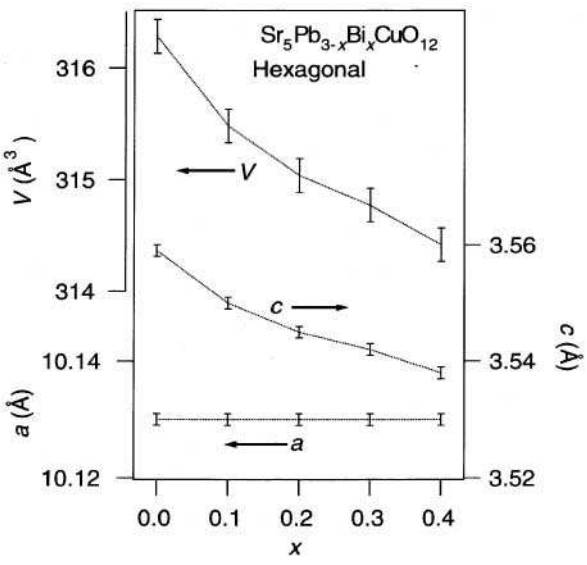

FIG. 1: Lattice constants and unit cell volume of $Sr_5Pb_{3-x}Bi_xCuO_{12}$ ($0 \leq x \leq 0.4$, $P\bar{6}2m$) measured by means of powder x-ray diffraction at room temperature.

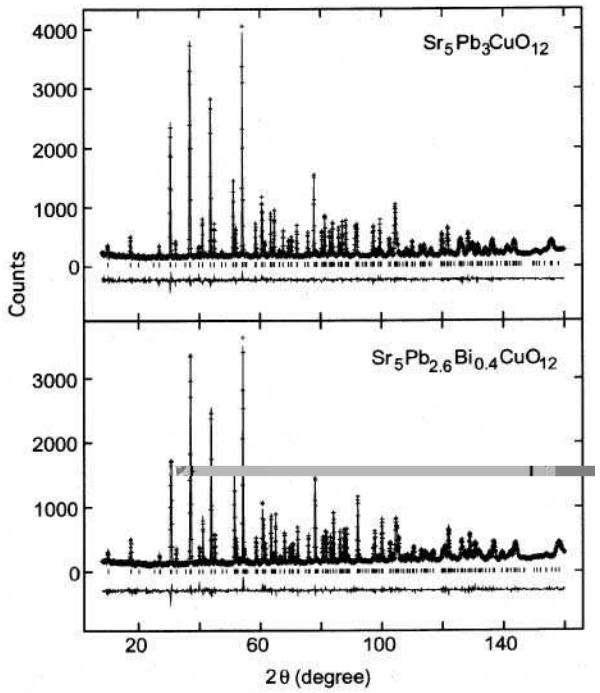

FIG. 2: Observed (crosses) and calculated (solid curve) powder neutron diffraction profiles (295 K) of $Sr_5Pb_3CuO_{12}$ and $Sr_5Pb_{2.6}Bi_{0.4}CuO_{12}$. The small vertical bars indicate calculated positions for the nuclear Bragg reflections. The lower part of each panel shows difference between the profiles.

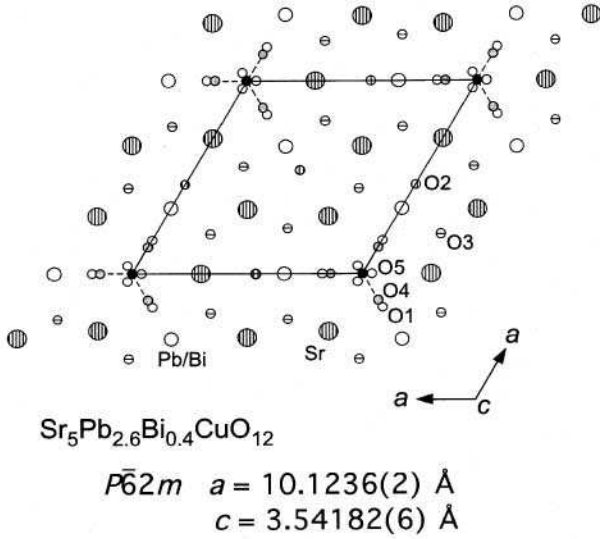

FIG. 3: Schematic crystal structure view for $Sr_5Pb_{2.6}Bi_{0.4}CuO_{12}$ drawn from the structure parameters at 295 K. The hexagonal unit cell is indicated by the solid lines. Copper ions are located at the corners of the unit cell in this view.

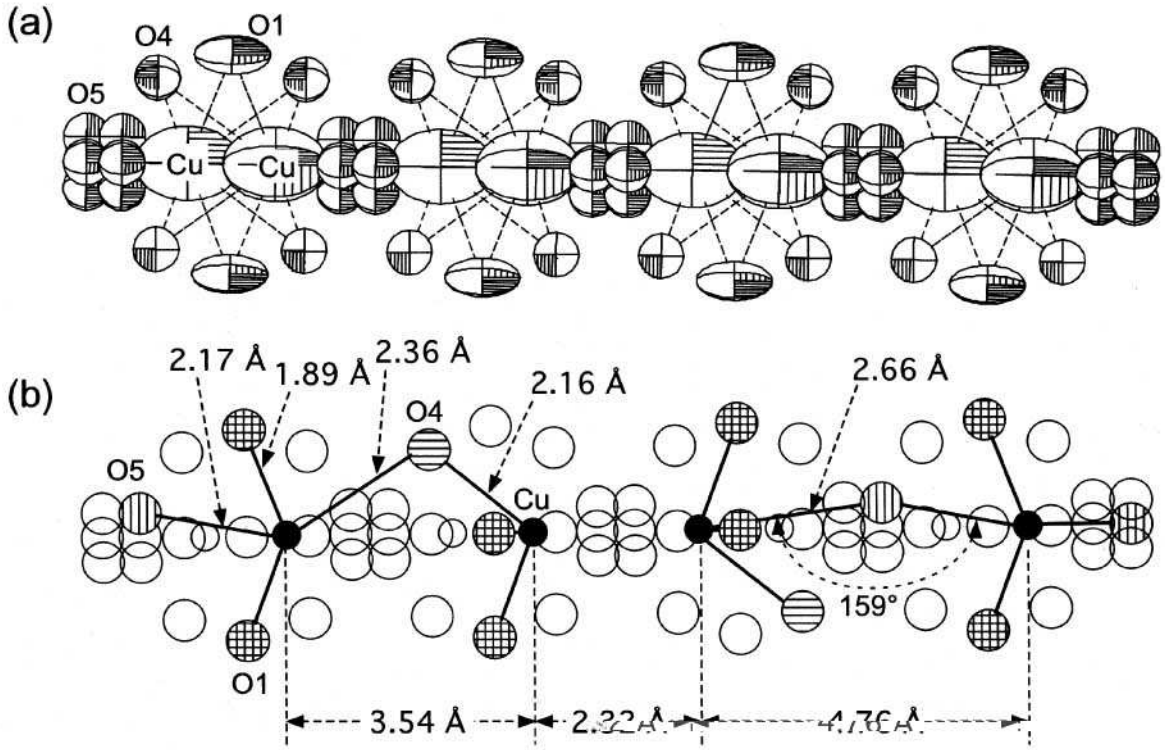

FIG. 4: (a) Schematic thermal ellipsoids view for the copper-oxygen chain along c–axis, drawn from the structure parameters of $Sr_5Pb_{2.6}Bi_{0.4}CuO_{12}$ at 295 K, showing the randomly occupied oxygen positions O(1), O(4) and O(5) around copper, (b) and a probable local coordination between copper and oxygen within the average structural model.

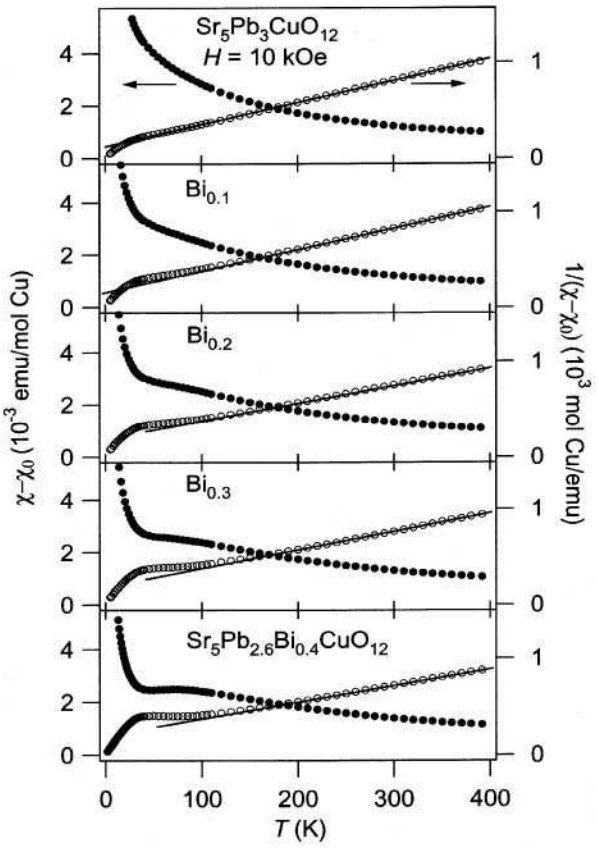

FIG. 5: Temperature dependence of magnetic susceptibility of $Sr_5Pb_{3-x}Bi_xCuO_{12}$ ($0 \leq x \leq 0.4$), and inverse plots of the susceptibility. The data were obtained at 10 kOe on heating after cooling each sample without the applied magnetic field. The solid lines indicate fits to the Curie-Weiss law.

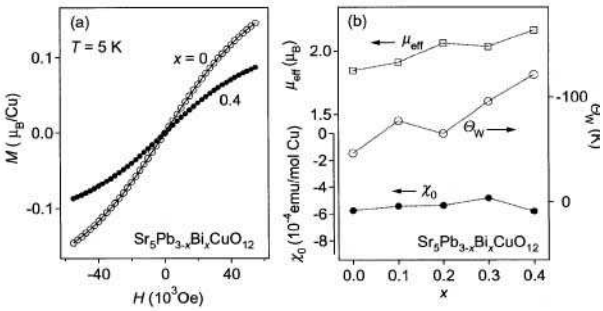

FIG. 6: Applied magnetic field dependence of magnetization of $Sr_5Pb_3CuO_{12}$ and $Sr_5Pb_{2.6}Bi_{0.4}CuO_{12}$ at 5 K. (b) Magnetic parameters of $Sr_5Pb_{3-x}Bi_xCuO_{12}$ ($0 \leq x \leq 0.4$) estimated by fitting the Curie-Weiss law to the magnetic susceptibility data.

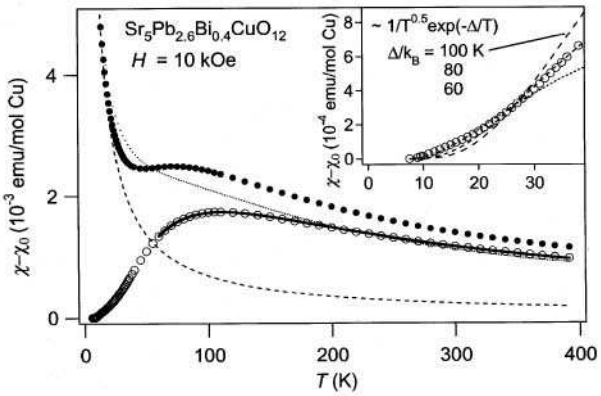

FIG. 7: Quantitative analysis of the magnetic susceptibility data of $Sr_5Pb_{2.6}Bi_{0.4}CuO_{12}$. The open circles result from subtraction of the low-temperature Curie component (broken curve, 13.3 % level) from original data (closed circles). Fat solid curve indicates a fit to alternating linear-chain model using a least squares method at $J_1/k_B = 183$ K, $\alpha = 0.58$, and $g = 2.22$. Inset: Estimation of magnitude of the possible magnetic gap by applying spin gap model [9], indicating it is approximately 80 K. Temporally applied an independent model, in which a linear relationship between Bonner-Fiser and Curie components exists, is indicated by dotted curve in the main panel.